Breakup of drops in a microfluidic T junction

A. M. Leshansky[a)] and L. M. Pismen
Department of Chemical Engineering, Technion, Haifa 32000, Israel

(Received 17 October 2008; accepted 5 January 2009; published online 25 February 2009)

We propose a mechanism of droplet breakup in a symmetric microfluidic T junction driven by pressure decrement in a narrow gap between the droplet and the channel wall. This mechanism works in a two-dimensional setting where the capillary (Rayleigh–Plateau) instability of a cylindrical liquid thread, suggested earlier [D. Link, S. Anna, D. Weitz, and H. Stone, Phys. Rev. Lett. **92**, 054503 (2004)] as the cause of breakup, is not operative, but it is likely to be responsible for the breakup also in three dimensions. We derive a dependence of the critical droplet extension on the capillary number Ca by combining a simple geometric construction for the interface shape with lubrication analysis in a narrow gap where the surface tension competes with the viscous drag. The theory, formally valid for $\mathrm{Ca}^{1/5} \ll 1$, shows a very good agreement with numerical results when it is extrapolated to moderate values of Ca. © *2009 American Institute of Physics*.
[DOI: 10.1063/1.3078515]

Much attention has been drawn recently to various droplet-based microfluidic techniques.[1,2] The use of droplets as "microreactors" offers many advantages in comparison with single-phase microfluidics, such as confinement of reactants or prevention of longitudinal dispersion and cross contamination between subsequent samples. Additional benefits might be reduction of unwanted adhesion/adsorption of the material confined in droplets at the channel walls and facilitated heat/mass transport due to enhanced internal mixing. Various techniques have been proposed and tested for production and manipulation of droplets and bubbles in a microfluidic format using "passive" control by externally driven flows that are varied locally by geometry of the channel in a continuous stream.[3–10]

One of the basic "unit operations" in droplet-based microfluidics concerns droplet/bubble *generation*[3,5,10,11] or *breakup*[8,9] in T-junction geometry. Droplets of controllable size can be formed when two immiscible fluids flow into a T junction through two inlet channels. On the other hand, droplets suspended in an immiscible carrier liquid break up into two smaller daughter droplets of highly controllable predetermined sizes as the droplet-laden flow enters a T junction through the inlet channel; after the breakup, each of the two daughter droplets follows the corresponding outlet channels.

In spite of a high interest to droplet-based microfluidic techniques, theoretical understanding of droplet formation and breakup in a T junction is quite limited. Link *et al.*[8] developed a scaling theory describing their experimental studies of droplet breakup in a symmetric (i.e., having daughter channels of equal lengths) T junction of a square cross section. The scaling of the droplet extension prior to breakup with the mean shear rate was based on the theory of unbounded axisymmetric extensional creeping flow past a viscous droplet,[12] while the observed critical size of a droplet at breakup was attributed to the capillary (Rayleigh–Plateau) instability of a long cylindrical liquid thread. This mechanism may be relevant at low surface tension (high capillary numbers) when conditions are similar to unconfined extensional flow. For a strongly confined geometry, at small or moderate capillary numbers, the breakup is more likely to be caused by an increased upstream pressure due to lubrication flow in a thin film sandwiched between the drop and the channel wall. This view has been, apparently, adopted in recent scaling theory of droplet formation in a T junction[10] and in flow-focusing geometry.[11] This is also supported by the results of numerical simulations of droplets in a T junction in two dimensions via volume-of-fluid (VoF) method combined with the interface reconstruction technique[13] (for details of the numerical scheme see Ref. 14). Not only that the observed breakup of a two-dimensional (2D) droplet resembles the breakup in three dimensions (see Fig. 1) but the location of the stability boundary separating breaking and nonbreaking drops in the applicable parametric plane (initial droplet extension versus capillary number) is in a close agreement in both 2D and three-dimensional (3D) cases, although capillary instability is, obviously, not operative in two dimensions.

Other arguments against the capillary instability scenario may be based on particular features of the observed droplet breakup. It is known that no finite mode of maximum instability is observed when viscosity is taken into account in the analysis of liquid thread stability.[15] This implies that the thread would not break up into droplets of size comparable to its circumference, which disagrees with experimental observations[8] where the incoming drop splits into two equal-sized drops in a symmetric T junction. Moreover, a liquid thread is unstable only to axisymmetric or varicose deformations, while it is stable to nonaxisymmetric deformations,[15] while deformation of the droplet in the T junction is nonaxisymmetric. All the above suggest that the droplet breakup is rather flow driven, similarly to a central pinch off of a droplet or a bubble in unbounded extensional flow, albeit more complicated due to confinement. The confinement is expected to play a predominant role in the dynamics of exten-

a)Electronic mail: lisha@technion.ac.il.

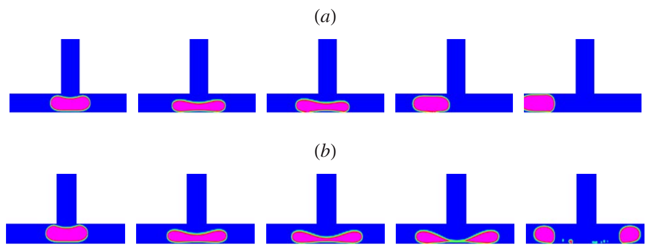

FIG. 1. (Color online) Snapshots of droplet shapes from 2D numerical simulations (Ref. 13). The time progresses from left to right: (a) a nonbreaking drop; (b) a breaking drop.

sion and breakup at high surface tension (low capillary number).

In the present work we propose a theory of droplet breakup in a symmetric T junction combining a simple geometric construction for the interface shape with lubrication analysis in a narrow gap between the droplet and channel wall. We study the 2D problem in the limit of small capillary numbers and assume that the pressure drop in the flow past a *stationary* droplet at the T junction (near breakup) is concentrated in a narrow gap region where lubrication approximation can be used.[16] Outside this region, the shape of the droplet is determined by surface tension alone, so that the droplet interface should be shaped as a circular arc with the curvature determined by the ambient pressure. Due to the pressure drop across the gap, the droplet should be convex at its outside tips and concave in the middle (depression) region. We shall see that it turns out to be impossible to attain a too high negative curvature at a fixed droplet volume. This leads to a critical condition determining droplet breakup.

Standard lubrication analysis of the flow in a thin stationary gap sandwiched between the droplet and the upper wall of the outlet channel (e.g., Ref. 17) yields the following equation for the gap thickness $h(x)$ as a function of the streamwise distance x (see Fig. 2):

$$h^3 h_{xxx} = \frac{3\mu v w}{\gamma}, \tag{1}$$

where v is the average fluid velocity in the daughter channel of width w,

$$v = w^{-1}\int_0^h u\,dy,$$

and γ stands for the interfacial tension. Thus, Eq. (1) can be rewritten as $h^3 h_{xxx}=3\text{Ca}w$, where Ca, $\text{Ca}=v\mu/\gamma$, is the capillary number.[18] The equation is formally valid in the gap region, and therefore we transform to "inner" dimensionless variables by scaling h with the unknown minimal gap thickness d and choosing the scale of x to eliminate Ca,

$$h = d\eta, \quad x = \frac{d^{4/3}}{w^{1/3}}(3\text{Ca})^{-1/3}\xi. \tag{2}$$

Under the chosen scaling (2), the nondimensional form of Eq. (1) reads

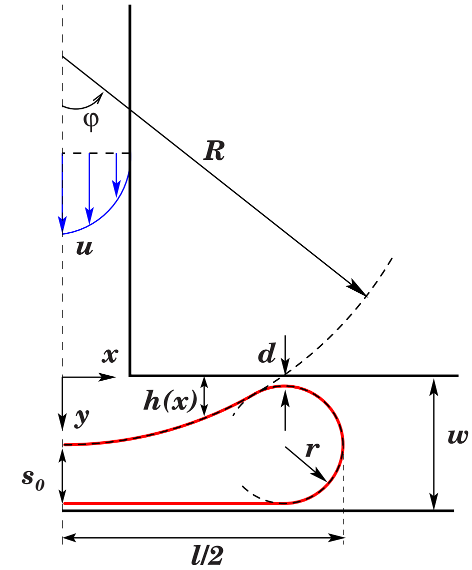

FIG. 2. (Color online) Schematic geometric construction for the equilibrium droplet shape; ℓ stands for the deformed droplet length, w is the width of the channel, R is the curvature radius of the depression region, φ is the polar angle counted from the symmetry axis, d is the thickness of the film sandwiched between the droplet and the channel wall, $r=(w-d)/2$ is the curvature radius at the tip, and s_0 is the width of the deformed drop at the symmetry axis.

$$\eta^3\eta'''(\xi) = 1. \tag{3}$$

Note that Eq. (3) is similar to the classical Landau–Levich–Bretherton equation[17] $\eta^3\eta'''(\xi)=\eta-1$ which, however, has a solution $\eta=1$ corresponding to a constant film thickness lacking in our case.

We are looking for solutions of Eq. (3) that satisfy $\eta(\xi^*)=1$ at the minimum of η, i.e., at $h=d$. For sufficiently small Ca, there is a region (near the droplet's tip) where $\eta=h/d\gg 1$, such that

$$\frac{dh}{dx} = \left(3\text{Ca}\frac{w}{d}\right)^{1/3}\frac{d\eta}{d\xi} \ll 1, \tag{4}$$

so that the lubrication approximation leading to Eq. (1) still holds. In this region, $\eta'''(\xi)\to 0$, and the curvature is almost constant, so that the shape is determined by surface tension alone. The order-of-magnitude estimate of the curvature behind the gap, which has to be matched to the curvature $\kappa=2/(w-d)$ at the droplet tip, is

$$\kappa = \frac{2}{w-d} = \frac{d^2h}{dx^2} \simeq K\frac{(3\text{Ca}w)^{2/3}}{d^{5/3}}, \tag{5}$$

where K is an $O(1)$ constant. Equation (5) gives the estimate of the minimal gap thickness, d/w, as a function of Ca. In the limit $d\ll w$, the result is

$$d/w \simeq (K/2)^{3/5}(3\text{Ca})^{2/5}. \tag{6}$$

The constant K has to be determined by numerical integration of Eq. (3) with some prescribed boundary conditions for $\eta''(\xi)$ and $\eta'(\xi)$ at $\xi=0$. Substituting the asymptotic scaling for the film thickness, Eq. (6), into Eqs. (4) and (5) yields

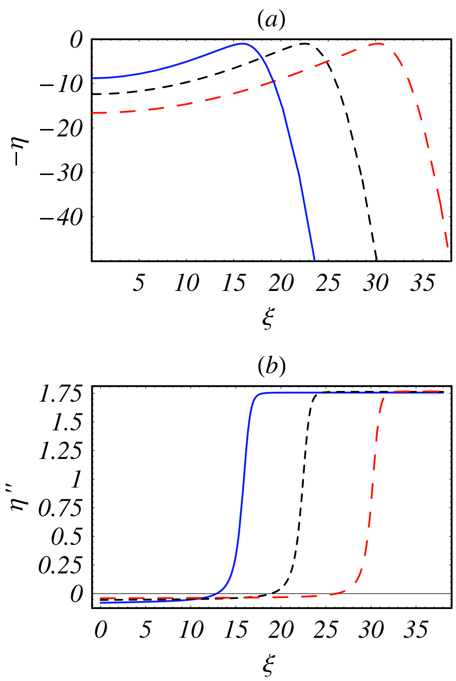

FIG. 3. (Color online) Numerical solution of the lubrication equation (3) with the boundary conditions $\eta'(0)=0$ and $\eta''(0)=-0.04$ (red, long dashes), $\eta''(0)=-0.055$ (black, short dashes), $\eta''(0)=-0.08$ (blue, solid): (a) the droplet shape $\eta(\xi)$; (b) the scaled curvature $\eta''(\xi)$.

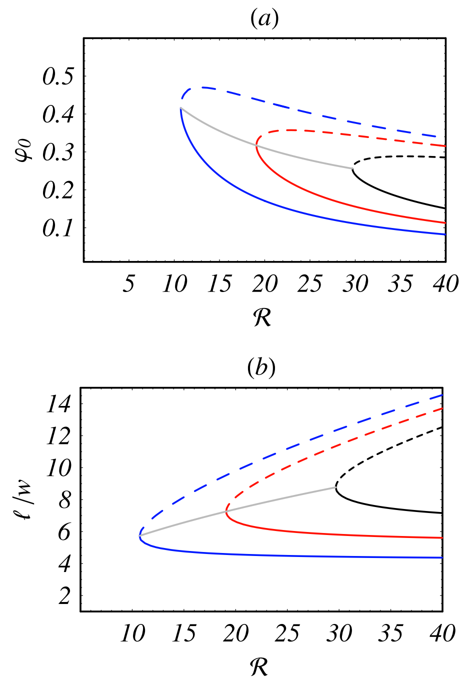

FIG. 4. (Color online) Graphical solution of Eq. (12) for $V=12$ (black, short dashes), $V=10$ (red, medium dashes), and $V=8$ (blue, long dashes). The lower branch corresponds to stable solutions and the solid gray lines connect the critical points: (a) the polar angle φ_0 plotted vs $\mathcal{R}$; (b) scaled elongation ℓ/w plotted vs $\mathcal{R}$.

$$\frac{dh}{dx} \simeq (6\text{Ca}\,K)^{1/5}\frac{d\eta}{d\xi}, \quad \frac{d^2h}{dx^2} \simeq \frac{2}{Kw}\frac{d^2\eta}{d\xi^2}. \tag{7}$$

Note that the lubrication approximation is applicable at $(3\text{Ca})^{1/5} \ll 1$, and therefore the theory is expected to be valid for rather small values of Ca. Equation (3) should be integrated in the direction of increasing ξ with some prescribed $\eta''(0)$ and $\eta'(0)$, fitting the value of $\eta(0)$ to attain the minimum thickness $\eta(\xi^*)=1$. The numerical integration has been performed in MATHEMATICA; the results are presented in Figs. 3(a) and 3(b). For small values of $-\eta''(0)$ corresponding to a large curvature radius of the concave region [see the analysis below leading to Eq. (16)], the solutions possess a nearly constant (negative) curvature in the depression region. Therefore we start integrating Eq. (3) from the symmetry axis with $\eta'(0)=0$. The resulting value of K is almost insensitive to the value of $\eta''(0)$ and changes in a narrow range between 1.74 and 1.76.

The dependence of the film thickness on Ca in Eq. (6) can be alternatively obtained from scaling arguments using a simple geometric construction. We approximate a 2D droplet by three joined shapes with constant curvatures: a central concave part and two symmetric circular arcs (see Fig. 2). The latter's radius is $r=(w-d)/2$, or approximately $w/2$ for $d \ll w$. The curvature radius of the concave region, R, is determined by the pressure drop in the carrier viscous liquid, which can be estimated using the lubrication approximation as $\Delta P = P_d^{(o)} - P_t^{(o)} \approx \mu v w l/d^3$, where l is the characteristic length scale of the lubricating film; the subscripts t and d stand for the tip and depression regions, respectively. The corresponding internal pressure within the deformed droplet at the depression is $P_d^{(i)} = P_d^{(o)} - \gamma/R$, and at the droplet tip, $P_t^{(i)} = P_t^{(o)} + 2\gamma/w$. The assumption of negligible pressure variation inside a low viscosity droplet (or a gas bubble) leads to the estimate

$$\gamma\left(\frac{1}{R}+\frac{2}{w}\right) \sim \frac{\mu v w l}{d^3}.$$

For the purpose of this estimate, one can approximate the shape of the interface in the gap by a circular arc with the radius $w/2$, and therefore $l \sim \sqrt{dw/2}$, which, together with $R \gg w/2$, yields the anticipated scaling, $d/w \sim \text{Ca}^{2/5}$.

In order to evaluate the volume constraint, we use the above geometric construction. We adopt the "outer" scaling, whereby the tip radius $r=(w-d)/2 \approx w/2$ is taken as unity, keeping in mind that it is identified with the principal geometric scale of the problem when the gap width is negligible. The vertical position z of the concave surface is defined by the equation

$$z(\varphi) = s_0 + \mathcal{R}(1-\cos\varphi), \tag{8}$$

where s_0 is the dimensionless minimal elevation, $\mathcal{R} = 2R/(w-d)$ is the dimensionless curvature radius of the concave region, and φ is the angle measured from the symmetry axis (see Fig. 2). The two arc shapes are joined at some elevation $z_0 = z(\varphi_0)$; they are joined smoothly when the angular position on the convex circular arc counted from its highest elevation point has the same value φ_0. The condition of equality of elevations on both arcs is

$$s_0 + \mathcal{R}(1-\cos\varphi_0) = 1 + \cos\varphi_0. \tag{9}$$

The dimensionless half-volume of the concave part is

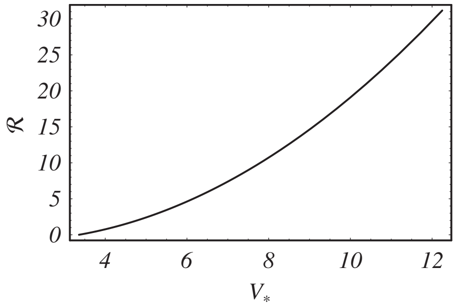

FIG. 5. Dimensionless curvature radius of the depression region $\mathcal{R}$ as a function of the dimensionless droplet volume V_* at the breakup threshold.

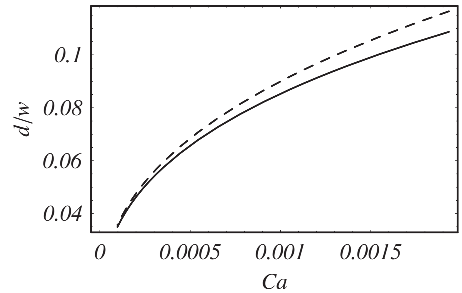

FIG. 7. The scaled minimal gap thickness d/w. The solid line corresponds to the solution of Eq. (5), while the dashed line is the asymptotic expression (6), $d/w \sim \mathrm{Ca}^{2/5}$, valid in the limit $d \ll w$.

$$V_1 = s_0 \mathcal{R} \sin \varphi_0 + \mathcal{R}^2\left(\sin \varphi_0 - \tfrac{1}{2}\varphi_0 - \tfrac{1}{4}\sin 2\varphi_0\right). \tag{10}$$

The dimensionless volume of either of the two convex parts is

$$V_2 = \sin \varphi_0 + \tfrac{1}{2}(\pi + \varphi_0) + \tfrac{1}{4}\sin 2\varphi_0. \tag{11}$$

Given the value of $\mathcal{R}$, we have to determine whether a composite shape satisfying the volume constraint does exist. Failure to meet the constraint signals the droplet breakup. This is determined by solving Eq. (9) together with the constraint $V = V_1 + V_2$, where V is the droplet half-volume and the functions $V_1(\varphi_0, s_0)$ and $V_2(\varphi_0)$ are defined by Eqs. (10) and (11) with respect of two unknowns s_0 and φ_0. The two equations are reduced by eliminating s_0 to a single equation,

$$\mathcal{R} - 1 - (\mathcal{R}+1)\cos \varphi_0 + \mathcal{R}^{-1} \times \left[\frac{\mathcal{R}^2 - 1}{2}\cos \varphi_0 - (\mathcal{R}^2 + 1) + \frac{(\mathcal{R}^2 - 1)\varphi_0 + 2V - \pi}{2 \sin \varphi_0}\right] = 0. \tag{12}$$

For any given volume V, this equation has two solutions at $\mathcal{R}$ exceeding a certain limit $\mathcal{R}_{\min}(V)$, i.e., when the pressure drop is below a critical value dependent on the droplet volume, and none otherwise [see Fig. 4(a)]. Of the two solution branches, the lower one, corresponding to positive s_0 over its entire length, is physical. The droplet half-length scaled with r, which is approximately equal (for small d) to the ratio of the droplet length to the channel width,

$$\ell/2r = (\mathcal{R}+1)\sin \varphi_0 + 1 \approx \ell/w, \tag{13}$$

grows on the physical branch with decreasing $\mathcal{R}$, until a maximum elongation is attained at the breaking point [see Fig. 4(b)].

The bifurcation point defining the droplet breakup is determined by vanishing derivative of the left-hand side of Eq. (12) with respect to φ_0, which yields

$$V_* = \tfrac{1}{2}[\pi - (\mathcal{R}^2 - 1)\varphi_0] - \tfrac{1}{4}(\mathcal{R}+1)\tan \varphi_0[1 - 3\mathcal{R} + (\mathcal{R}+1)\cos 2\varphi_0]. \tag{14}$$

This bifurcation point marks the highest pressure drop at which a droplet of a given volume may exist; the critical radius grows, and, consequently, the critical pressure drop decreases with growing volume.

Using $V = V_*$ in Eq. (12) simplifies the relation on the lower branch to

$$\mathcal{R} = \frac{\cos \varphi_0}{1 - \cos \varphi_0}. \tag{15}$$

This, together with Eq. (9), results in $s_0 = 1$ at the breakup threshold, which, in the dimensional form, yields the maximum elevation $(w-d)/2 \approx w/2$. The relations (14) and (15) define in a parametric form the dependence $V_*(\mathcal{R})$ shown in Fig. 5.

It should be noted that, although the curve in Fig. 5 continues formally to $\mathcal{R}=0$, only solutions with $\mathcal{R} \geqslant 1$ are physically admissible, since otherwise the convex interface

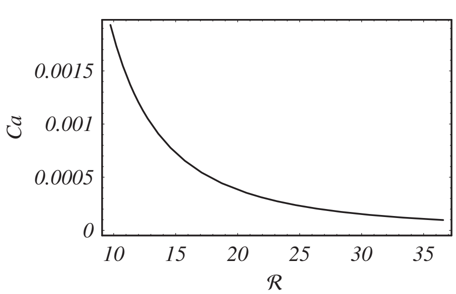

FIG. 6. The dependence of capillary number Ca on the dimensionless curvature radius of the depression region $\mathcal{R}$.

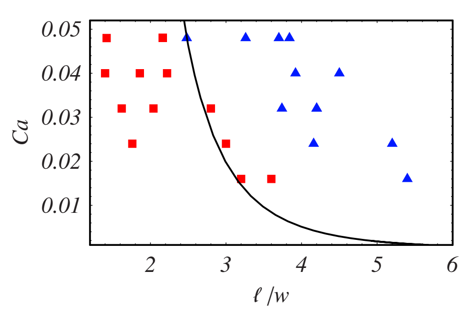

FIG. 8. (Color online) Maximum extension of the 2D droplet as a function of Ca. The solid line is the theoretical prediction extrapolated to moderate values of Ca, $\ell/w \simeq 1.3\ \mathrm{Ca}^{-0.21}$. The symbols correspond to the results of 2D VoF simulations (Ref. 13): breaking drops (▲) and nonbreaking drops (■).

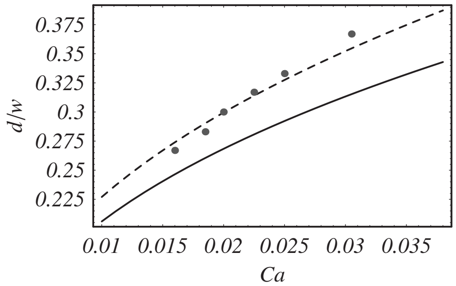

FIG. 9. Comparison of the film thickness dependence on Ca between the prediction of the low Ca theory (solid line) and the thin-gap-estimate equation (6) (dashed line) with the numerical simulations (symbols) for nonbreaking drops for a range of Ca between 0.016 and 0.031 outside the formal validity of the present theory. Each point stands for the results of several simulations for the same Ca but upon varying elongation.

encroaches upon the central region beyond the gap. This dependence is translated into a dependence $V_*(\mathrm{Ca})$ with the help of the lubrication solution in the gap region. The dimensionless curvature radius $\mathcal{R}$ is matched to $\eta''(0)$, taken as a boundary condition in the gap computation via the second equation of Eq. (7),

$$\frac{1}{\mathcal{R}} \simeq \frac{\eta''(0)}{K}. \tag{16}$$

The corresponding value of Ca is determined using Eqs. (2) and (6) by setting $\eta(0)$ equal to the critical elevation $s_0 \approx 1$ rescaled to the gap units, i.e., $\eta(0) \simeq K^{-3/5}(6\mathrm{Ca})^{-2/5}$. The resulting dependence of Ca on $\mathcal{R}$ is shown in Fig. 6.

Having Ca and K at hand, we can also compute the minimum dimensionless gap thickness d/w as a function of Ca using Eq. (5). This dependence is depicted in Fig. 7 (solid line), while the dashed line corresponds to the approximate solution (6) valid for $d \ll w$. The dependence $V_*(\mathrm{Ca})$ can be transformed into the dependence of the dimensionless elongation ℓ_0/w on Ca similar to Fig. 2(k) of Ref. 8. Alternatively, the critical extension of the droplet at the breakup threshold, ℓ/w, can be computed using Eq. (13) corrected for the finite gap width $d \sim \mathrm{Ca}^{2/5}$. We plot in Fig. 8 the resulting dependence extrapolated to moderate values of Ca, together with the simulation results[13] corresponding to the breakup of low viscosity (with the viscosity ratio of 0.125) 2D drops. The agreement between the theoretical prediction, $\ell/w \simeq 1.3\ \mathrm{Ca}^{-0.21}$, and the numerical results is very good, even though the theory is formally valid at values Ca rather lower than those explored numerically. The weak dependence of the critical extension on the capillary number, i.e., $\ell/w \sim \mathrm{Ca}^{-1/5}$, is in accord with experimental results in Ref. 8 where it was found that ℓ/w was nearly constant ($\sim\pi$).

The minimal film thickness estimate (6) emerging from the *local* analysis of the lubrication flow in a thin film sandwiched between the nonbreaking drop and the wall of the daughter channel is compared to the results of the VoF simulations in Fig. 9. It is readily seen that the agreement between the two is very good even at moderate Ca and relatively thick gaps outside the formal validity of the theory. Please note that no adjustable parameter is involved in this comparison.

To conclude, we developed 2D theory of the droplet breakup in a symmetric T junction. The dependence of the critical droplet extension on the capillary number Ca has been derived by combining a simple geometric construction for the interface shape with lubrication analysis in a narrow gap where the surface tension and viscous forces are comparable. The extension to the 3D case is possible, though the analogous geometric construction of a 3D droplet is more complicated. Note that for a 3D droplet, the anticipated pressure drop due to the lubrication flow in a thin film is less severe, since only a part of the carrier liquid flows through the film, whereas some fluid may escape through the corners of the microchannel. Our analysis cannot be extended in a straightforward way to asymmetric T junctions (i.e., having daughter channels of different hydraulic resistance) where the breakup process (producing two unequal drops) is intrinsically dynamic, being dominated by the mean flow direction. For instance, it was recently demonstrated in experiments on droplet generation in a two inlet T junction[10] that low capillary number breakup is solely controlled by the flow rate ratio of the two phases.

We would like to thank Patrick Tabeling for sharing with us unpublished experimental results. A.M.L. acknowledges the support of the Israel Science Foundation (ISF) (Contract Number 890014). L.M.P. acknowledges the support by the Minerva Center for Nonlinear Physics of Complex Systems.

[1] H. A. Stone, A. D. Stroock, and A. Ajdari, "Engineering flows in small devices: Microfluidics toward a lab-on-a-chip," Annu. Rev. Fluid Mech. **36**, 381 (2004).
[2] V. Cristini and Y. C. Tan, "Theory and numerical simulation of droplet dynamics in complex flows—a review," Lab Chip **4**, 257 (2004).
[3] T. Thorsen, R. W. Roberts, F. H. Arnold, and S. R. Quake, "Dynamic pattern formation in a vesicle-generating microfluidic device," Phys. Rev. Lett. **86**, 4163 (2001).
[4] S. Sugiura, M. Nakajima, S. Iwamoto, and M. Seki, "Interfacial tension driven monodispersed droplet formation from microfabricated channel array," Langmuir **17**, 5562 (2001).
[5] J. D. Tice, H. Song, A. D. Lyon, and R. F. Ismagilov, "Formation of droplets and mixing in multiphase microfluidics at low values of the Reynolds and the capillary numbers," Langmuir **19**, 9127 (2003).
[6] P. B. Umbanhowar, V. Prasad, and D. A. Weitz, "Monodisperse emulsion generation via drop break off in a coflowing stream," Langmuir **16**, 347 (2000).
[7] M. Prakash and N. Gershenfeld, "Microfluidic bubble logic," Science **315**, 832 (2007).
[8] D. R. Link, S. L. Anna, D. A. Weitz, and H. A. Stone, "Geometrically mediated breakup of drops in microfluidic device," Phys. Rev. Lett. **92**, 054503 (2004).
[9] Y. C. Tan, J. S. Fisher, A. I. Lee, V. Cristini, and A. Phillip, "Design of microfluidic channel geometries for the control of droplet volume, chemical concentration, and sorting," Lab Chip **4**, 292 (2004).
[10] P. Garstecki, M. J. Fuerstman, H. A. Stone, and G. M. Whitesides, "Formation of droplets and bubbles in a microfluidic T-junction—Scaling and mechanism of break-up," Lab Chip **6**, 437 (2006).
[11] B. Dollet, W. van Hoeve, J.-P. Raven, P. Marmottant, and M. Versluis, "Role of the channel geometry on the bubble pinch-off in flow-focusing devices," Phys. Rev. Lett. **100**, 034504 (2008).
[12] Y. Navot, "Critical behavior of droplet breakup in axisymmetric viscous flow," Phys. Fluids **11**, 990 (1999).
[13] P. Urbant, "Numerical simulations of drops in microchannels," M.S. thesis, Technion, 2006.
[14] P. Urbant, A. Leshansky, and Yu. Halupovich, "On the forced convective heat transport in a droplet-laden flow in microchannels," Microfluid. Nanofluid. **4**, 533 (2008).

[15]S. Chandrasekhar, *Hydrodynamic and Hydromagnetic Stability* (Dover, New York, 1981).
[16]Recent experimental work [M.-J. Tsang M. Ching, M.-C. Jullien, C. Cohen, L. Menetrier and P. Tabeling, "Droplet break-up in microfluidic T-junction at small capillary numbers," Phys Fluids (unpublished)] suggests that for small capillary numbers, Ca $<10^{-3}$, the breakup is intrinsically dynamic, as the droplet ruptures before reaching a steady shape. In this sense, the theory described in the present paper refers to the regime they identify as "shear-driven breakup."
[17]F. Bretherton, "The motion of long bubbles in tubes," J. Fluid Mech. **10**, 166 (1961).
[18]The capillary number, as defined in this paper, is based on the average velocity in the outlet channel. Note that usually it is based on average velocity in the inlet channel.